Concise Report

Analytical methods, NMR spectroscopy, t_1 noise suppression, Resampling, Compressed sensing

CJC Chinese Journal of Chemistry 中国化学 An International Journal

REAL-t_1, an Effective Approach for t_1-Noise Suppression in NMR Spectroscopy Based on Resampling Algorithm

Linhong Song,[‡,a,b] Jiannan Wang,[‡,a,b] Xuncheng Su,[c] Xu Zhang,[a,b] Conggang Li,[a,b] Xin Zhou,[a,b] Daiwen Yang,[d] Bin Jiang,*[,a,b] and Maili Liu*[,a,b]

[a] *State Key Laboratory of Magnetic Resonance and Atomic and Molecular Physics, Wuhan National Laboratory for Optoelectronics, National Center for Magnetic Resonance in Wuhan, Key Laboratory of Magnetic Resonance in Biological Systems, Wuhan Institute of Physics and Mathematics, Chinese Academy of Sciences, Wuhan, Hubei 430071, China*

[b] *University of Chinese Academy of Sciences, Beijing 100049, China*

[c] *State Key Laboratory of Elemento-Organic Chemistry, Collaborative Innovation Center of Chemical Science and Engineering, College of Chemistry, Nankai University, Tianjin 300071, China*

[d] *Department of Biological Sciences, National University of Singapore, 14 Science Drive 4, Singapore 117543, Singapore*

Cite this paper: *Chin. J. Chem.* **2020**, *38*, 77—81. **DOI: 10.1002/cjoc.201900389**

Summary of main observation and conclusion In multidimensional (*n*D) NMR spectroscopy, t_1 noise usually appears as ridges along indirect dimensions, and affects observation of weak signals. The main source of t_1 noise is instrumental instability, which causes random variation of FID amplitude during data acquisitions and introduces random noise-like peaks into spectrum after Fourier transformation. A number of efforts have been devoted, in order to develop new method or to improve existing approaches for suppressing t_1 noise. Herein, we propose a novel t_1 noise suppression method based on resampling algorithm for data processing, shortened as REAL-t_1. The method was verified using simulated 2D spectra, and NOESY spectra of sucrose and protein GB1, showing that the spectral quality was improved in all cases. The performance of REAL-t_1 was also compared with another recently proposed method, which showed that these two methods provided similar performance while REAL-t_1 cost much shorter experimental time.

Background and Originality Content

NMR spectroscopy can provide rich information of molecular structure, interaction and dynamics at atomic resolution, and has been intensively used in many fields such as chemistry, biology, and medicine. That information is generally obtained from multidimensional (*n*D) NMR spectra/experiments, where the inherent artifacts, such as t_1 noise,[1-2] truncation,[3-4] *etc*., often deteriorate quality of spectra and subsequently hinder correct derivation of qualitative and quantitative information. The t_1 noise appears as ridges of noise parallel to the indirect dimension associated with strong peaks in *n*D spectra, and especially the NOE based experiments suffer the most. The phenomena of t_1 noise were noticed about forty years ago[5-7] and the sources were analyzed soon after.[1-2] Since then, there has been a continuous interest in developing methods for t_1 noise suppression, which may be summarized into three categories: application of pulsed field gradient (PFG), experimental design and post-processing. In the first category, application of PFG is well known for coherence pathway selection and is improved as a simple way in t_1 noise suppression.[8-20] It was also demonstrated that p-type signals have less t_1 noise than n-type signals in PFG-COSY.[20] The experimental design, the second category, mainly focuses on reducing intense diagonal peaks that t_1 noise is associated with,[21-25] and on elimination of the t_1 noise by means of randomized acquisition in the indirect dimension[26] or temperature control.[27] We had shown that PFG, double quantum filter and diagonal free COSY could dramatically reduce the t_1 noise.[23] In the third category, symmetrization of 2D spectrum was proposed by Wüthrich *et al*. in 1981.[28] The methods based on subtraction or weighted smoothing were also proposed to reduce t_1 ridges.[22,29-30] The other post-processing methods include reference deconvolution,[31] correlated trace denoising[32] and singular value decomposition.[33] Recently, it was reported that co-addition of multiple spectra could reduce t_1 noise significantly, due to that t_1 noise from different acquisition is unlikely to correlate with each other.[34]

We had proposed an effective method[35-36] for simultaneously suppressing non-uniform sampling artifacts and noise in NMR spectroscopy based on resampling algorithm (REAL)[37] and compressed sensing.[38] And this method was implemented most recently in protein crystallography, to suppress spurious peaks and non-correlative noises in the difference Patterson maps.[39] Considering the random feature of the t_1 noise,[1-2,34] this method is extended as an alternative approach for suppressing t_1 noise. The proposed technique REAL-t_1, standing for t_1 noise suppression by resampling algorithm, was verified with simulated and experimental data. The improved spectral qualities are obtained in all cases.

Results and Discussion

The procedure of REAL-t_1 processing is diagramed in Figure 1. The initial spectrum (B_0), is obtained conventionally from the sampled raw time domain dataset (A_0). If spectrometer is not stable enough, t_1 noise associated with strong peak will be presented in the spectrum B_0. In the next step, a number of sub-datasets (A_1, A_2, ⋯, A_n) are randomly selected from A_0 using the resampling principle.[37] In order to get a reliable noise-suppressed spectrum, the number of generated sub-datasets should be more than 40, and the size of sub-dataset should be between 50% and 65% of the data points of the raw time domain dataset.[35] More sub-datasets may bring higher statistical precision, but take longer processing time. And according to our experience, the number of sub-datasets higher than 100 does not improve processing performance obviously. These sub-datasets are non-uniformly sampled (NUS) data, in which case compressed sensing method (CS)[38] is chosen for spectral reconstruction from the sub-datasets, resulting in the same number of sub-spectra or testing spectra (B_1,

*E-mail: jbin@wipm.ac.cn (Bin Jiang), ml.liu@wipm.ac.cn (Maili Liu)

‡ The authors with equal contribution.

For submission: https://mc.manuscriptcentral.com/cjoc

For articles: https://onlinelibrary.wiley.com/journal/16147065

B_2, ⋯, B_n). It has been demonstrated that CS is able to remove the artifacts induced by non-uniform sampling.[40-43] As demonstrated, t_1 noise is differently distributed in the testing spectra (B_1, B_2, ⋯, B_n), while the true signal peaks appear steadily. The reason is that, t_1 noise is actually caused by random variation of FID, and each sub-dataset has different FID combination. Thus, the statistics of spectral intensity fluctuation among testing spectra is able to distinguish between true signals and t_1 noise. In the third step, relative standard variations (RSD) were obtained for every spectral elements based on the statistical analyses. The true signals should have small RSD, while t_1 noise should have large RSD. Thus, the RSD is used to distinguish signals/peaks and t_1 noise. Next, a weighting matrix (D, in Figure 1) is generated from RSD matrix by equation (1), where α defines noise level in the resulting spectrum, β is the jump sharpness of weighting function curve, and ε is related to the RSD threshold to differentiate true signal and t_1 noise.[35] As the final step, the noise suppressed spectrum (Figure 1C) is derived by point-by-point multiplication of the initial spectrum (B_0) and the weighting matrix (D).

$$w = \alpha + \frac{1-\alpha}{1+e^{\beta\cdot(RSD-\varepsilon)}} \quad (1)$$

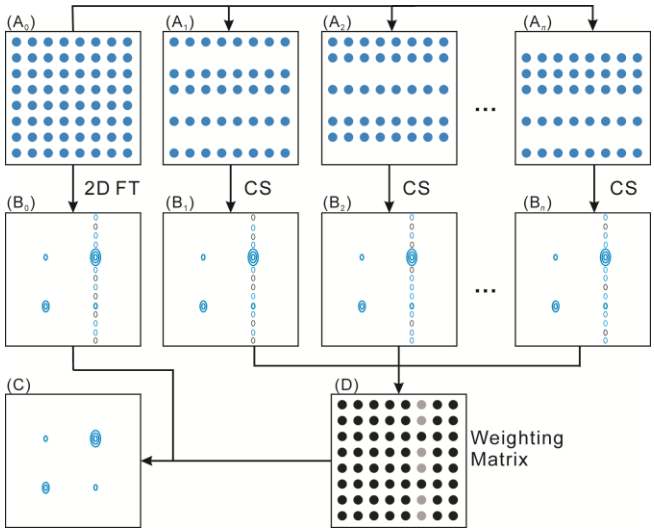

Figure 1 The scheme of REAL-t_1 processing method.

The performance of REAL-t_1 was verified using simulated data firstly. A simulated 2D time domain dataset was constructed using the parameters shown in Table 1. This dataset was processed conventionally to obtain a spectrum without t_1 noise, as shown in Figure 2A. The simulated t_1 noise was introduced into Figure 2B by randomly adjusting the FID amplitude of each t_1 increment,[33] since the main source of t_1 noise is the instrument instability among scans. The REAL-t_1 processed spectrum was shown in Figure 2C, in which t_1 noise was well suppressed. For comparison, the spectra co-addition method proposed by Mo *et al.*[34] was applied by addition of eight simulated spectra with t_1 noise generated in the same manner stated above, and the result is shown in Figure 2D. Although both methods give rise to similar results in t_1 noise suppression, the spectra co-addition method needs at least eight independently sampled datasets as the authors suggested, which means it costs much more experimental time than REAL-t_1.

Table 1 Line parameter values of the simulated spectrum (t_1 noise free)

Peak index	Resonance frequency/Hz		Amplitude	Transverse relaxation rate/s^{-1}
	F_1	F_2		
1	–30	–30	12 000	4
2	–30	30	70	4
3	30	–30	70	4
4	30	30	200	4

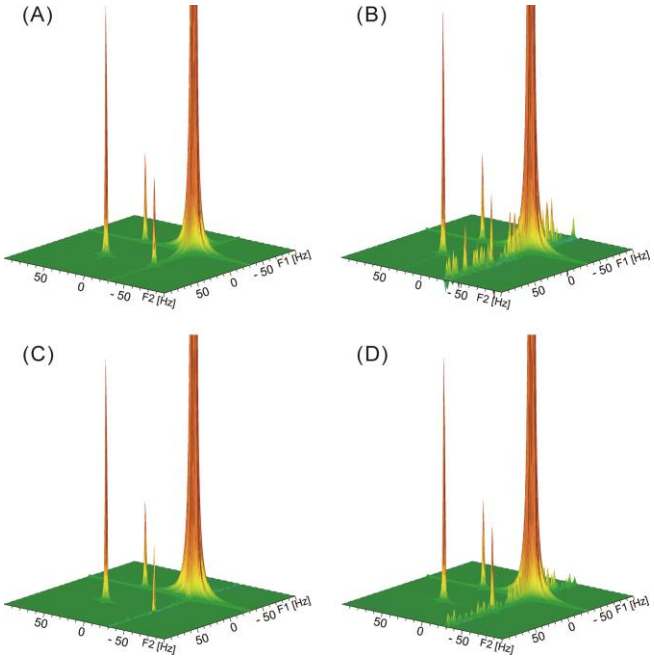

Figure 2 (A) The simulated 2D NMR spectrum according to the parameters in Table 1. (B) The spectrum introduced t_1 noise by randomly adjusting the FID amplitude of each t_1 increment. (C) The t_1 noise suppression with REAL-t_1 method. (D) The t_1 noise suppression by addition of eight independently simulated spectra.

For the above simulated datasets, the spectral width was 200 Hz in each dimension, and the sampling complex points were 256 and 512 in t_1 and t_2 dimensions, respectively. When introducing t_1 noise, the random adjusting of FID amplitude was performed by multiplication with a scaling factor randomly distributed between 0.95 and 1. In the conventional processing of the simulated data, squared cosine was used as window function in both dimensions. The sizes of processed data were extended to 512 and 1024 in t_1 and t_2 dimensions by zero filling. In the resampling procedure of REAL-t_1 processing, there were 65 sub-datasets randomly chosen from the original dataset, and every sub-dataset contained 60% data points. For each sub-dataset, after normal processing performed in t_2 dimension, t_1 data points were reconstructed by iterative soft threshold (IST) method, which is a commonly used compressed sensing reconstruction algorithm,[42-43] then they were processed conventionally to obtain testing spectrum. In the generation of weighting matrix, the values of α, β and ε of Eq. (1) were 0.1, 100, and 0.2, respectively.

The proposed method was also verified by NOESY spectra of small organic molecule sucrose and protein GB1. Figures 3A and 4A showed the original NOESY spectra of sucrose and GB1, respectively. As marked with red rectangles in Figure 3A, there was apparent t_1 noise near δ 3.6 and δ 3.74 (F_2). As shown in Figure 3B, t_1 noise was well suppressed by REAL-t_1 processing. When the spectrum was added with another seven independently sampled spectra,[34] t_1 noise was suppressed to the similar extent, as demonstrated in Figure 3C. The similar performances of REAL-t_1 and spectra co-addition method were also observed in t_1 noise suppression on the NOESY spectra of GB1, as shown in Figures 4B and 4C.

The sucrose sample was 5 mg sucrose dissolved in 0.6 mL D_2O. The NOESY experiment of sucrose was performed on a Bruker AVANCE III 600 spectrometer. The spectral width was 2000 Hz for both F_1 and F_2 dimensions. The size of sampled complex points

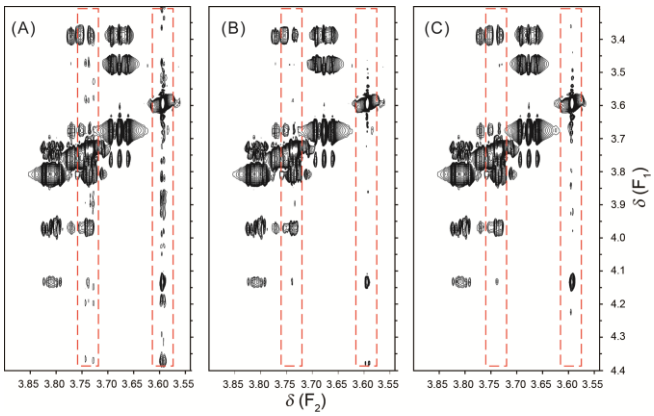

Figure 3 Part of the NOESY spectra of sucrose. As marked with red rectangles, there was obvious t_1 noise near δ 3.6 and δ 3.74 (F2) in (A) the original spectrum. The t_1 noise was suppressed by (B) REAL-t_1 processing, and by (C) co-addition of eight independently sampled spectra.

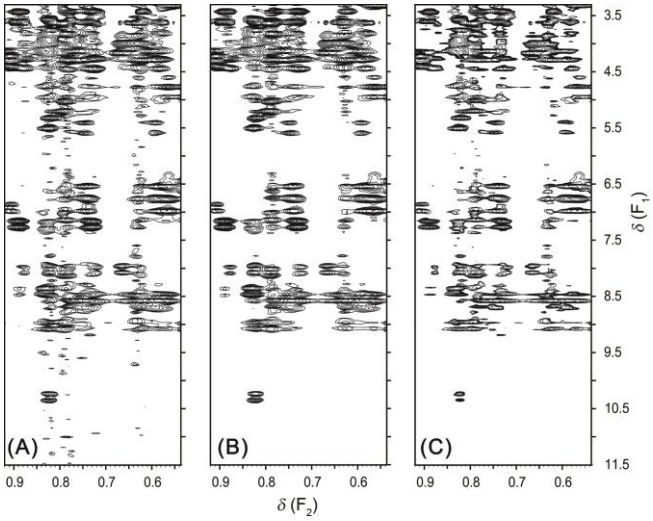

Figure 4 Part of the NOESY spectra of protein GB1. (A) The original spectrum in which there was t_1 noise near δ 0.8 and δ 0.64 (F2). (B) The t_1 noise suppression by REAL-t_1 processing. (C) The t_1 noise suppression by co-addition of eight independently sampled spectra.

was 128 (t_1) by 1024 (t_2). The weighting function was squared cosine for both dimensions. The size of time domain dataset was extended to 256 (t_1) by 2048 (t_2) by zero filling. In REAL-t_1 processing, the parameters were the same with those in the former REAL-t_1 processing on simulated data. The protein sample was a 5 mM aqueous solution (10% D_2O) of 15 N labeled GB1. The NOESY experiment of GB1 was performed on a Bruker AVANCE III 800 spectrometer. The spectral width was 12820 Hz for both F_1 and F_2 dimensions. The size of sampled complex points was 256 (t_1) by 1024 (t_2). The weighting function was squared cosine for both dimensions. The size of time domain dataset was extended to 512 (t_1) by 2048 (t_2) by zero filling. In REAL-t_1 processing, there were 90 sub-datasets randomly chosen from the original dataset, and every sub-dataset contained 65% data points. In the generation of weighting matrix, the values of α, β and ε of Eq. (1) were 0.1, 100, and 0.5, respectively. The concentration of GB1 sample was much lower than that of sucrose, thus, more sub-datasets and more data points in each sub-dataset were needed for enough signal-to-noise ratios in the REAL-t_1 processing on GB1 NOESY spectrum.

The parameters used in REAL-t_1 processing certainly influence the quality of processed spectrum. To explore the parameter set-up, one signal and three t_1 noise peaks were arbitrarily selected respectively from the previous sucrose NOESY and GB1 NOESY spectra. These peaks were marked in the Supporting Information. When the number of resampled sub-datasets was set from 10 to 140 with increment 10, the RSD values of those selected peaks were plotted in Figure 5. As shown in this figure, the RSD values of t_1 noise peaks fluctuated largely in case of small sub-dataset number, and the fluctuation of RSD values tended to convergence when the number of sub-datasets increased. Since RSD value is the critical criterion to distinguish true signal and t_1 noise, larger sub-dataset number will bring more stable processing performance. From Figure 5, when sub-dataset number was larger than 40, RSD fluctuation decreased, and when sub-dataset number was larger than 100, RSD fluctuation became flat. Thus, in REAL-t_1 processing, the number of sub-datasets should be higher than 40 at least. And for stable performance, it is recommended to set sub-dataset number around 100 or higher. Certainly more sub-datasets need more processing time, so it has to compromise between performance and processing time. From Figure 5, the RSD of t_1 noise peaks were all higher than 0.6 when the RSD variation stabilized. It is also found in Figure 5 that, the RSD of true signal in (B) the GB1 NOESY was much higher than that in (A) the sucrose NOESY. This phenomenon was caused by the different signal to noise ratio (SNR) in these two spectra. Due to the low solute concentration, signals in the GB1 NOESY spectrum were influenced by background noise (thermal noise), which resulted in higher signal RSD in the GB1 NOESY spectrum. The distribution of RSD in Figure 5(B) indicated that setting ε as 0.5 is recommended for low SNR spectra. The quantitative relation between SNR and signal RSD in REAL-t_1 processing will be studied in further work.

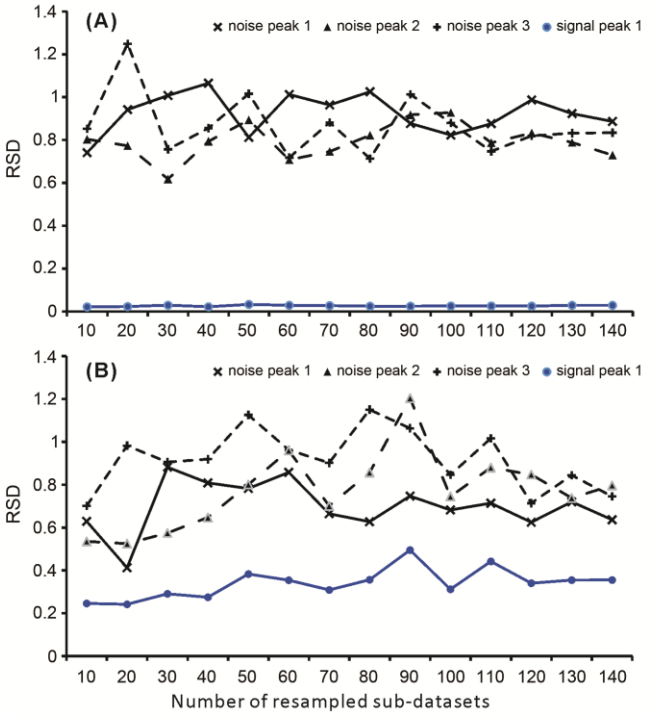

Figure 5 The RSD curves of signal and t_1 noise peak intensities with number of resampled sub-datasets. The RSD values of one signal peak and three t_1 noise peaks of (A) the sucrose NOESY spectrum and (B) the GB1 NOESY spectrum, were ploted with the number of resampled sub-datases in REAL-t_1 processing. The locations of those signal and t_1 noise peaks were listed in the Supporting Information.

The simulated data was generated using a home-made MATLAB script. The conventional processing of the simulated and experimental data was performed with NMRPipe.[44] The software used to perform REAL-t_1 processing, was made up of Python

scripts, NMRPipe scripts, and C++ programs. All the above mentioned scripts and programs are available upon request from the authors.

Conclusions

A statistical resampling based processing method called REAL-t_1 was proposed to suppress t_1 noise in multidimensional NMR experiments. Its performance was verified by simulated data, and NOESY spectra of small molecule sucrose and protein GB1. Compared with the recently reported spectra co-addition method,[34] REAL-t_1 provided similar t_1 noise suppression performance with much less experimental time.

Supporting Information

The processing performance of REAL-t_1 on an HSQC spectrum of the mixture of sortase A protein and QALPETG-NH2 peptide. The locations of selected signal and t_1 noise peaks observed in Figure 5. The Supporting Information for this article is available on the WWW under https://doi.org/10.1002/cjoc.201900389.

Acknowledgement

This work is supported by grants from the National Key R&D Program of China (Nos. 2018YFA0704002, 2018YFE0202300, 2017YFA0505400), the National Natural Science Foundation of China (Nos. 21735007, 21675170, 21475146), and the Chinese Academy of Sciences (QYZDJ-SSW-SLH027).

References

[1] Mehlkopf, A. F.; Korbee, D.; Tiggelman, T. A.; Freeman, R. Sources of t1 noise in two-dimensional NMR *J. Magn. Reson.* **1984**, *58*, 315–323.
[2] Morris, G. A. Systematic sources of signal irreproducibility and t1 noise in high-field NMR spectrometers *J. Magn. Reson.* **1992**, *100*, 316–328.
[3] Lindon, J. C.; Ferrige, A. G. Digitization and data-processing in Fourier-transform NMR *Prog. Nucl. Magn. Reson. Spectrosc.* **1980**, *14*, 27–66.
[4] Jiang, B.; He, X. M.; Yang, Y. H.; Zhang, X.; Zhou, X.; Li, C. G.; Yang, D. W.; Liu, M. L. Suppress Sampling Truncation Artifacts in Constant-time Type Nuclear Magnetic Resonance Experiments Using Iterative Soft Thresholding Method. *Chin. J. Anal. Chem.* **2017**, *45*, 1888–1894.
[5] Nagayama, K.; Bachmann, P.; Wuthrich, K.; Ernst, R. R. Use of cross-section and of projections in 2-dimensional NMR spectroscopy. *J. Magn. Reson.* **1978**, *31*, 133–148.
[6] Levitt, M. H.; Freeman, R. Phase adjustment of 2-dimensional NMR spectra. *J. Magn. Reson.* **1979**, *34*, 675–678.
[7] Hall, L. D.; Sukumar, S. Phase-sensitive displays for proton 2D-J spectra. *J. Magn. Reson.* **1980**, *38*, 555–558.
[8] Crouch, R. C.; Davis, A. O.; Martin, G. E. Pure absorption phase gradient-enhanced HMQC-TOCSY with direct response editing. *Magn. Reson. Chem.* **1995**, *33*, 889–892.
[9] Crouch, R. C.; Martin, G. E. Long-range H1-N15 correlation at natural abundance using gradient-enhanced inverse-detection. *J. Heterocycl. Chem.* **1995**, *32*, 1665–1669.
[10] Bauer, W. Pulsed field gradient 'inverse' HOESY applied to the isotope pairs H-1,P-31 and H-1,Li-7. *Magn. Reson. Chem.* **1996**, *34*, 532–537.
[11] Van, Q. N.; Shaka, A. J. Improved cross peak detection in two-dimensional proton NMR spectra using excitation sculpting. *J. Magn. Reson.* **1998**, *132*, 154–158.
[12] Dalvit, C.; Bohlen, J. M. Evaluation of the performance of 2D H-1 PFG absorption mode DQ spectroscopy in the analysis of chemical and biological molecules. *Magn. Reson. Chem.* **1998**, *36*, 670–680.
[13] Lin, G. X.; Liao, X. L.; Lin, D. H.; Zheng, S. K.; Chen, Z.; Wu, Q. Y. t(1) noise and sensitivity in pulsed field gradient experiments. *J. Magn. Reson.* **2000**, *144*, 6–12.
[14] Reynolds, W. F.; Enriquez, R. G. Gradient-selected versus phase-cycled HMBC and HSQC: pros and cons. *Magn. Reson. Chem.* **2001**, *39*, 531–538.
[15] Alam, T. M.; Pedrotty, D. M.; Boyle, T. J. Modified, pulse field gradient-enhanced inverse-detected HOESY pulse sequence for reduction of t(1) spectral artifacts. *Magn. Reson. Chem.* **2002**, *40*, 361–365.
[16] Gaede, H. C.; Gawrisch, K. Multi-dimensional pulsed field gradient magic angle spinning NMR experiments on membranes. *Magn. Reson. Chem.* **2004**, *42*, 115–122.
[17] Willker, W.; Leibfritz, D. Determination of heteronuclear long-range H,X coupling constant from gradient-selected HMBC spectra. *Magn. Reson. Chem.* **1995**, *33*, 632–638.
[18] Horne, T. J.; Morris, G. A. Combined use of gradient-enhanced techniques and reference deconvolution for ultralow t(1) noise in 2D NMR spectroscopy. *J. Magn. Reson., Ser A* **1996**, *123*, 246–252.
[19] Heikkinen, S.; Rahkamaa, E.; Kilpelainen, I. Use of RF gradients in excitation sculpting, with application to 2D HSQC. *J. Magn. Reson.* **1997**, *127*, 80–86.
[20] Horne, T. J.; Morris, G. A. P-type gradient-enhanced COSY experiments show lower t(1) noise than N-type *Magn. Reson. Chem.* **1997**, *35*, 680–686.
[21] Denk, W.; Wagner, G.; Rance, M.; Wuthrich, K. Combined suppression of diagonal peaks and t1 ridges in two-dimensional nuclear overhauser enhancement spectra. *J. Magn. Reson.* **1985**, *62*, 350–355.
[22] Glaser, S.; Kalbitzer, H. R. Improvement of two-dimensional NMR spectra by weighted mean t1-ridge subtraction and antidiagonal reduction. *J. Magn. Reson.* **1986**, *68*, 350–354.
[23] Liu, H. L.; Jiang, B.; Liu, M. L.; Mao, X. A. Fast nuclear magnetic resonance correlation spectroscopy without diagonal peaks: The "2-1" correlation spectroscopy. *Rev. Sci. Instrum.* **2008**, *79*, 026104.
[24] Robertson, A. J.; Pandey, M. K.; Marsh, A.; Nishiyama, Y.; Brown, S. P. The use of a selective saturation pulse to suppress t(1) noise in two-dimensional H-1 fast magic angle spinning solid-state NMR spectroscopy. *J. Magn. Reson.* **2015**, *260*, 89–97.
[25] Perras, F. A.; Pruski, M. Reducing t1 noise through rapid scanning. *J. Magn. Reson.* **2019**, *298*, 31–34.
[26] Bowyer, P. J.; Swanson, A. G.; Morris, G. A. Randomized acquisition for the suppression of systematic F-1 artifacts in two-dimensional NMR spectroscopy. *J. Magn. Reson.* **1999**, *140*, 513–515.
[27] Bowyer, P. J.; Swanson, A. G.; Morris, G. A. Analyzing and correcting spectrometer temperature sensitivity. *J. Magn. Reson.* **2001**, *152*, 234–246.
[28] Baumann, R.; Wider, G.; Ernst, R. R.; Wuthrich, K. Improvement of 2D NOE and 2D correlated spectra by triangular multiplication. *J. Magn. Reson.* **1981**, *44*, 402–406.
[29] Klevit, R. E. Improving two-dimensional NMR spectra by t1 ridge subtraction. *J. Magn. Reson.* **1985**, *62*, 551–555.
[30] Manoleras, N.; Norton, R. S. Spectral processing methods for the removal of t1 noise and solvent artifacts from NMR spectra. *J. Biomol. NMR* **1992**, *2*, 485–494.
[31] Gibbs, A.; Morris, G. A.; Swanson, A. G.; Cowburn, D. Suppression of t1 noise in 2D-NMR spectroscopy by reference deconvolution. *J. Magn. Reson., Ser A* **1993**, *101*, 351–356.
[32] Poulding, S.; Charlton, A. J.; Donarski, J.; Wilson, J. C. Removal of t(1) noise from metabolomic 2D H-1-C-13 HSQC NMR spectra by Correlated Trace Denoising. *J. Magn. Reson.* **2007**, *189*, 190–199.
[33] Brissac, C.; Malliavin, T. E.; Delsuc, M. A. Use of the Cadzow procedure in 2D NMR for the reduction of t(1) noise. *J. Biomol. NMR* **1995**, *6*, 361–365.
[34] Mo, H. P.; Harwood, J. S.; Yang, D. Z.; Post, C. B. A simple method for NMR t(1) noise suppression. *J. Magn. Reson.* **2017**, *276*, 43–50.
[35] Jiang, B.; Luo, F.; Ding, Y. M.; Sun, P.; Zhang, X.; Jiang, L.; Li, C. G.; Mao, X. A.; Yang, D. W.; Tang, C.; Liu, M. L. NASR: An Effective Ap-

proach for Simultaneous Noise and Artifact Suppression in NMR Spectroscopy. *Anal. Chem.* **2013**, *85*, 2523–2528.
[36] Nie, L.; Jiang, B.; Zhang, X.; Liu, M. A Compressed Sensing and Resampling Based Noise Suppression Method for NMR. *Chin. J. Mang. Reson.* **2016**, *33*, 244–256.
[37] Good, P. I. *Resampling Methods: A Practical Guide to Data Analysis*, 3rd ed., Birkhauser, Boston, **2006**.
[38] Candes, E. J.; Romberg, J. K.; Tao, T. Stable signal recovery from incomplete and inaccurate measurements. *Commun. Pure Appl. Math.* **2006**, *59*, 1207–1223.
[39] Hu, M.; Gao, Z.; Zhou, Q.; Geng, Z.; Dong, Y. A noise and artifact suppression using resampling (NASR) method to facilitate de novo protein structure determination. *Radiat. Det. Tech. Meth.* **2019**, *3*, 48.
[40] Holland, D. J.; Bostock, M. J.; Gladden, L. F.; Nietlispach, D. Fast Multidimensional NMR Spectroscopy Using Compressed Sensing. *Angew. Chem. Int. Ed.* **2011**, *50*, 6548–6551.
[41] Kazimierczuk, K.; Orekhov, V. Y. Accelerated NMR Spectroscopy by Using Compressed Sensing. *Angew. Chem. Int. Ed.* **2011**, *50*, 5556–5559.
[42] Bostock, M. J.; Holland, D. J.; Nietlispach, D. Compressed sensing reconstruction of undersampled 3D NOESY spectra: application to large membrane proteins. *J. Biomol. NMR* **2012**, *54*, 15–32.
[43] Hyberts, S. G.; Milbradt, A. G.; Wagner, A. B.; Arthanari, H.; Wagner, G. Application of iterative soft thresholding for fast reconstruction of NMR data non-uniformly sampled with multidimensional Poisson Gap scheduling. *J. Biomol. NMR* **2012**, *52*, 315–327.
[44] Delaglio, F.; Grzesiek, S.; Vuister, G. W.; Zhu, G.; Pfeifer, J.; Bax, A. NMRPIPE - a multidimensional spectral processing system based on UNIX pipes. *J. Biomol. NMR* **1995**, *6*, 277–293.

Manuscript received: September 30, 2019
Manuscript revised: October 30, 2019
Manuscript accepted: November 12, 2019
Accepted manuscript online: November 14, 2019
Version of record online: December 3, 2019

